

Predicting Critical Transitions From Time Series Synchronphasor Data

Eduardo Cotilla-Sanchez, *Member, IEEE*, Paul D. H. Hines, *Member, IEEE*, and Christopher M. Danforth

Abstract—The dynamical behavior of power systems under stress frequently deviates from the predictions of deterministic models. Model-free methods for detecting signs of excessive stress before instability occurs would therefore be valuable. The mathematical frameworks of “fast-slow systems” and “critical slowing down” can describe the statistical behavior of dynamical systems that are subjected to random perturbations as they approach points of instability. This paper builds from existing literature on fast-slow systems to provide evidence that time series data alone can be useful to estimate the temporal distance of a power system to a critical transition, such as voltage collapse. Our method is based on identifying evidence of critical slowing down in a single stream of synchronized phasor measurements. Results from a single machine, stochastic infinite bus model, a three machine/nine bus system and the Western North American disturbance of 10 August 1996 illustrate the utility of the proposed method.

Index Terms—Criticality, power system monitoring, synchronized phasor measurements.

I. INTRODUCTION

I NCREASING evidence suggests that electric power systems frequently operate near critical points at which a small disturbance could trigger instability. The disturbances of, for example, 14 August 2003 and 8 September 2011 in North America [1], [2], 4 November 2006 in Europe [3] and 10 November 2009 in South America [4] accentuate the continuing need for new technology that can warn operators when a power system approaches critical operating points.

Many changes in which a power system moves from a stable, secure operating state to one that could result in degraded network performance can be studied using the framework of critical transitions. Voltage collapse, for example, can be described as a saddle-node bifurcation [5]. Small-signal instability typically results in critically- or under-damped oscillations, which can be understood using the theory of Hopf bifurcations [6].

Manuscript received November 24, 2011; revised March 28, 2012; accepted July 23, 2012. This work was supported in part by the U.S. Department of Energy under Award DE-OE0000447, and in part by the U.S. National Science Foundation under Award ECCS-0848247. Paper no. TSG-00654-2011.

E. Cotilla-Sanchez is with the School of Electrical Engineering and Computer Science, Oregon State University, Corvallis, OR 97331 USA (e-mail: cotillaj@eeecs.oregonstate.edu).

P. Hines is with the School of Engineering, University of Vermont, Burlington, VT 05405 USA (e-mail: paul.hines@uvm.edu).

C. M. Danforth is with the Department of Mathematics and Statistics, Vermont Complex Systems Center, Vermont Advanced Computing Core, University of Vermont, Burlington, VT 05405 USA (e-mail: chris.danforth@uvm.edu).

Color versions of one or more of the figures in this paper are available online at <http://ieeexplore.ieee.org>.

Digital Object Identifier 10.1109/TSG.2012.2213848

There is a long history of using eigenvalue analysis to evaluate these types of critical transitions. Extensive research shows that the eigenvalues of the linearized system equations can be used to predict proximity to voltage collapse and small-signal instability [7]–[12]. Recent research [13] shows that linearization can be avoided by using the nonlinear Koopman operator to estimate the proximity of a system to critical points. However, accurately estimating eigenvalue (or mode) trajectories in a large system requires accurate models and large quantities of sensor data.

The parameters in most power system models naturally include some error, particularly in the ways that bordering balancing areas affect the area being modeled. Furthermore, random fluctuations, such as from noisy loads or variable sources like wind and solar, can affect system dynamics in ways that are not captured by standard eigenvalue analysis methods. Methods that can identify emerging risks without detailed network models may be helpful in such cases. With the deployment of synchronized phasor measurement units (PMUs or synchronphasors) operators have increasing access to large quantities of high-resolution, time-synchronized data. Methods that can turn these data into information about operating risk, without relying on network models, could dramatically increase the value of synchronphasor technology, and help operators to make better decisions about when or if to implement risk mitigating operating procedures.

A number of methods for estimating blackout risk from phase-angle data exist in the power systems literature. Recent advances in the use of PMU data are described in [14]–[16]. [17] describes a method for measuring phase differences between groups of generators from time series data. Relatedly, [18] describes a method for estimating voltage differences between areas based on PMU measurements and circuit theory. In [19], the authors illustrate how to calculate stability margins utilizing a “ball-on-concave-surface” dynamic equivalent. Other methods that extract frequency information from PMU data are described in [20]–[24]. Some of these approaches proved useful for tracking the progression of slow oscillations [21] and the assessment of post-fault stability [24].

This paper takes a somewhat different approach by building on recent research in the area of nonlinear stochastic dynamical systems, which shows that large, complex systems frequently show evidence of “critical slowing down” (CSD) before they reach points of critical transition [25]. We leverage the methods described in [25], [26] to obtain metrics that use a single time series of PMU data and appear to provide a strong indication of proximity to system failure. Results from a single machine stochastic infinite bus power system model, a three machine, nine bus power system model, and data from the 10 August

1996 blackout in the Western North American interconnection indicate that there is substantial information regarding system health in even a single stream of PMU data.

The remainder of this paper is organized as follows. Section II provides a summary of the mathematical framework of fast-slow critical transitions that underly the methods proposed in this paper. Section III describes our adaption of these concepts to the task of measuring critical slowing down in a power system. Section IV discusses the results obtained from three test systems. Lastly, Section V discusses the implications of this work.

II. CRITICAL TRANSITIONS AND FAST-SLOW SYSTEMS

Numerous recent articles suggest that the properties of data from stochastic dynamical systems can be used to signal the proximity of a system to a tipping point, catastrophic shift, or critical transition. This section discusses how these results may be useful for predicting critical transitions in power systems.

A dynamical system described by differential equations experiences a *bifurcation* when a change in its parameters provoke a qualitative change in the motion of the system. Some bifurcations are benign, such as the transition from a state with over-damped oscillations (complex eigenvalues in the left-half plane) to a state with over-damped exponential recovery. In this case the stability of the system is not compromised. However, other bifurcations result in instability. *Critical bifurcations* (or critical transitions) of this sort result in a shift from a stable regime to an unstable one. Systems that undergo a critical transition will settle (if at all) at a point that is far from the original equilibrium operating state. This paper focuses on identifying proximity of a power system to critical transition.

Physical systems are constantly subject to stochastic forcings that perturb the system state from its attractor. While random perturbations can excite instabilities in a system, they can also produce statistical patterns that provide early-warning signs of proximity to critical transition. Several recent articles show that statistical patterns emerge in time series data from a variety of complex systems before they reach a critical transition (see the review in [25]). Examples in which such early warning signs appear include ecosystem models before extinction [27], climate models before abrupt climate change [26], the human body before an epileptic seizure [28], and financial markets before a collapse [29]. These examples suggest a type of universality in the dynamics of stochastic complex systems. In each case, time-domain measurements taken from the system before the transition show the following statistical patterns:

- 1) increased recovery times from perturbations;
- 2) increased signal variance from the mean trajectory;
- 3) increased flicker and asymmetry (increased kurtosis) in the signal.

Together, these properties are commonly referred to as “critical slowing down” (CSD), a phenomenon originally observed in models of emergent magnetic fields in ferro-magnetic materials [30]. As described in [25], these three properties can be identified by statistical tests for increasing variance and autocorrelation (or autoregression) in time series measurements taken from the system.

A. Fast-Slow Systems

The mathematical framework of fast-slow systems provides some explanation for why variance and autocorrelation increase in stochastic differential systems before critical transitions occur. A fast-slow system is one that can be described by two sets of ordinary differential equations (ODE): one that moves slowly toward a critical point, and the other that has shorter time constants [31]. Equation (1) is the general form for a system with a fast variable (or vector) u , and a slow one v :

$$\begin{cases} \dot{u} = f(u, v) \\ \dot{v} = \epsilon g(u, v). \end{cases} \quad (1)$$

In (1) ϵ is a small parameter ($0 < \epsilon \ll 1$) that makes v vary slowly relative to the shorter time variation in u . In a power system ϵ might represent, for instance, the rate at which a load gradually increases toward voltage collapse. Interactions between the dynamics of the fast subsystem (u) and the slowly varying variables (v) can precipitate a critical transition away from a stable operating point.

Many critical bifurcations can be classified as either fold, Hopf, Pitchfork, or transcritical. Fold (or saddle node) and Hopf bifurcations are particularly relevant to power systems because they can be used to describe common instabilities such as voltage collapse and the onset of oscillatory behavior. In the following paragraphs we review common, simplified examples (known as the “normal forms,” adapted from [31], [32]) that illustrate the properties of fold and Hopf bifurcations.

A system with a *fold bifurcation* has two stable operating points, which gradually approach one another as the slow variable (v) increases. When the two operating points collide, the two equilibrium conditions are eliminated, resulting in an unstable system. Voltage collapse is a familiar example of a fold bifurcation. Equation (2) illustrates a simple two-variable fast-slow fold bifurcation, with a critical transition when the slow variable v reaches zero.

$$\begin{cases} \dot{u} = -v - u^2 \\ \dot{v} = \epsilon g(u, v). \end{cases} \quad (2)$$

An example of a simple power system that exhibits a fold bifurcation is the single machine infinite bus (SMIB) [33]. In the baseline SMIB model that we use in this paper the generator is located at Bus 1, with terminal voltage $V_1 = |V_1| e^{i\theta_1}$. The generator is a lossless round rotor, and produces $P_e(t)$ electric power as a result of $P_m(t)$ mechanical forcing. The generator has a constant field voltage magnitude (E_a) behind a synchronous reactance (X_d). The rotor dynamics are governed by the classic swing equation [34] with $P_e(t)$ subject to the network equations for this specific circuit:

$$P_m(t) = P_e(t) + D\dot{\delta}(t) + M\ddot{\delta}(t) \quad (3)$$

$$P_e(t) = \frac{E_a V_2(t)}{X_d + X_{12}} \sin(\delta(t)) \quad (4)$$

where $\delta(t)$ is the machine rotor angle, relative to the phase angle of the infinite bus ($\theta_2 = 0$), D and M are machine damping and inertia constants and X_{12} is the reactance of the transmission line between the two buses. From (4) it is clear that the SMIB model becomes unstable when P_m

reaches $|E_q|V_2(t)/X_d + X_{12} = P_{\max}$. When $P_m < P_{\max}$ there are two equilibrium solutions for δ that satisfy (4). With $P_m \geq P_{\max}$ the system Jacobian becomes singular, and the system unstable. For a detailed discussion of this model, see [33]. Section IV-A discusses an extension of the SMIB model to a stochastic case.

In a *Hopf bifurcation*, a system with exponential recovery rates transitions to one in which oscillations are critically- or under-damped; i.e., a pair of real-valued and negative eigenvalues become a complex conjugate pair with non-negative real parts. Equation (5), from [35], describes such a system:

$$\begin{cases} \dot{u}_1 = vu_1 - u_2 + \lambda_1 u_1 (u_1^2 + u_2^2) \\ \dot{u}_2 = u_1 + vu_2 + \lambda_1 u_2 (u_1^2 + u_2^2) \\ \dot{v} = \epsilon g(u, v) \end{cases} \quad (5)$$

where λ_1 is the first Lyapunov coefficient. [36], [37] discuss ways in which Hopf bifurcations appear in the SMIB model, after adding an exciter, for various combinations of D and P_m .

In summary, there is extensive literature showing that many types of power system instability can be understood using (2) and (5). Numerous bifurcation analyses in the power system literature expand on the two examples described above and study transitions (including Pitchfork and transcritical bifurcations) that result from the introduction of more detailed component models, such as generator exciters and limiters (e.g., [5], [8], [33], [36]–[38]). Many of these analyses are reviewed in the IEEE/PES committee report [39].

B. Stochastic Fast-Slow Systems

The above examples show critical transitions as they move smoothly past the critical point (at $v = 0$). Real systems, however, are subject to random external fluctuations that can substantially change the dynamical properties of the critical transitions [40]. The theory of fast-slow stochastic differential equations (fast-slow SDEs) can provide formal insight into the behavior of stochastic systems as they approach critical transition. SDEs are challenging because with the introduction of noise, not only do systems inherit the deterministic bifurcations from the original ODEs, but they also show “noise-induced transitions,” which were not present in the deterministic system. If the magnitude of the noise is small relative to the variance of the process, the stochastic transitions occur in the neighborhood of the corresponding deterministic transitions [31]. When the noise is larger, transitions can occur at many locations.

The following example, similar to those derived in [31], [32], illustrates how a relatively simple fast-slow SDE show signs of critical slowing down when approaching a tipping point. Let us consider the stochastic extension of (2) with one fast variable ($u \in \mathbb{R}^1$) and one slow variable ($v \in \mathbb{R}^1$) with a bifurcation at $v = 0$:

$$\begin{cases} du = (-v - u^2) dt + \sigma dW_t \\ dv = \epsilon dt \end{cases} \quad (6)$$

where $\sigma > 0$ is a constant and W_t is a Wiener process. [31] shows that solving (6) for the probability density function (pdf) of u , for a given v , is

$$p(u = U|v) = 1 \mathcal{C} e^{2\sigma^2(-vU - 1/3 U^3 + 2/3(-v)^3)^2} \quad (7)$$

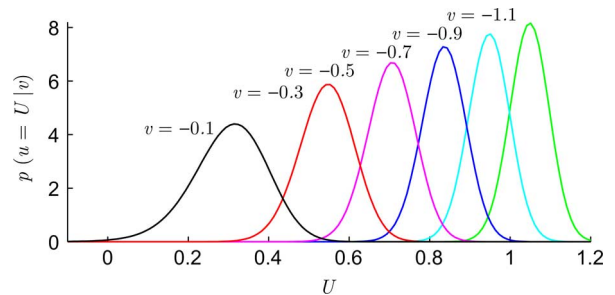


Fig. 1. Probability density functions for the random variable u in (6) and (7), for different values of v as it increases toward the critical transition at $v = 0$. As v increases toward the critical point, the variance in u increases.

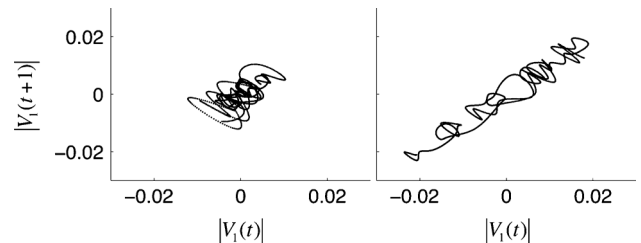


Fig. 2. An illustration of increasing autocorrelation and variance in generator bus voltages $|V_1|$ (after subtracting the mean) in a stochastic SMIB model. The left panel compares voltage changes, with a one second time delay, in an unstressed regime. The right panel shows time-delayed voltage deviations shortly before the critical transition (see Section IV-A).

where \mathcal{C} is a normalization constant that depends on the boundary points chosen to solve the Fokker-Planck equation resulting from (6) and evaluated around the singular limit $\epsilon \rightarrow 0$. Plotting this pdf (Fig. 1), we see that as v approaches the bifurcation at $v = 0$ the variance in the random signal u increases. [32] demonstrates that for a given realization of this process (ξ) with additive noise, the variance scales as:

$$\text{Var}(\xi) = \sigma^2 \left[\mathcal{O}_v \left(\frac{1}{\sqrt{v}} \right) + \mathcal{O}(\epsilon) \right] + \mathcal{O}(\sigma^4). \quad (8)$$

Therefore, holding all other things constant, the signal variance will increase with $v^{-1/2}$ near the critical transition. Using simulations, [31], [32] also show that autocorrelation in u increases as the system approaches the critical transition. Fig. 2 illustrates this increase in autocorrelation for a stochastically forced version of the SMIB model (see Section IV-A). Because this same pair of trends is apparent in many large complex systems [25] we conjecture that increasing signal autocorrelation and variance will provide early warning of critical transitions in a variety of power system models.

In large power systems the stochastic differential-algebraic equations (SDAEs) are sufficiently large and uncertain to make analytical solutions, such as (7), impractical. [41] shows that under some conditions one can linearize the system equations and use Itô calculus to solve the stochastic ODEs to obtain estimates of proximity to critical bifurcations. However, this approach remains computationally expensive, and relies on network models that are not perfectly accurate. The results from stochastic fast-slow systems indicate that there is significant information about proximity to critical transition in raw time series data, which can be extracted with minimal computational effort and is insensitive to modeling errors. A more formal and comprehensive review of the link between power system ODEs

and stochastic fast-slow systems is a valuable direction for future work, given that some of the theoretical results that we discuss in this section are still being developed within the applied mathematics literature.

III. METHODS: MEASURING CRITICAL SLOWING DOWN

Given that critical slowing down (CSD), as evidenced by an increase in signal variance and autocorrelation, can provide an early warning for critical transitions, we need good methods to detect statistically significant increases in these measures. This section describes a procedure for detecting statistically significant CSD in a signal. Our method is an adapted version of the procedure in [26], which was used to measure proximity to transition in global climate models. The following steps summarize the proposed procedure for identifying CSD in any time domain signal $x(t)$. In our examples we replace $x(t)$ with streams of voltage magnitude $|V(t)|$, phase angle $\theta(t)$ or frequency $\omega(t)$ measurements.

- 1) *Choose a window size (T)* within which to test for autocorrelation and variance. This window should be large enough to minimize the impact of spurious changes in the signal and to include multiple periods from signal frequencies that might be indicators of stress (common oscillatory modes, for example), yet small enough such that changes in the signal do not become excessively averaged. In this paper we use a 2-minute window size. In the appendix we show that the quality of our proximity indicator is quite robust to changes in T .
- 2) *Detrend the signal.* Filter the data in each window to remove slow trends that are not the result of CSD. This detrending should, for example, remove slow changes in phase angles due to gradual changes in system load. Following the method in [26] we use a low-pass filter based on a Gaussian Kernel Smoothing (GKS) function to capture the dc and low-frequency portions of x within the window, and then subtract the filtered signal from the original (10). The smoothing comes from convolving the sampled signal $x[k]$ with a discretized Gaussian function:

$$h(n, \sigma_f) = \frac{1}{\sqrt{2\pi}\sigma_f} e^{-n^2/2\sigma_f^2} \quad (9)$$

where σ_f determines the bandwidth of the filter and n is an index for the number of samples from the origin. σ_f should be chosen to ensure that only the dc component and very gradual trends remain in the filtered signal GKS (x). The final detrended signal $d(x) = d[k]$ is the difference between the original and the filtered signal:

$$d(x) = x[k] - \text{GKS}(x[k]). \quad (10)$$

For the results in this paper we use $\sigma_f = 5$ or $\sigma_f = 10$. In the appendix we show that the results are not highly sensitive to the choice of σ_f . Experimental results indicate that the GKS detrending technique is effective in removing gradual trends in the data. However, it is important to note that there are likely to be many detrending methods that are similarly effective for this step in the algorithm (see, e.g., [42]).

- 3) *Measure for autocorrelation.* In this paper we assume that $x(t)$ has been sampled at 30 Hz (as is common for processed PMU data), which means that consecutive samples $d[k]$ and $d[k - 1]$ are separated by 1/30 s. As in [26], we fit an auto-regressive (AR) model of order 1 (11) to the detrended, discretized signal $d[k]$:

$$d[k] = a_1 d[k - 1] + e[k]. \quad (11)$$

The AR coefficient a_1 , is found by minimizing the error term $e[k]$, using the ordinary least squares method. Because $x[k]$ is detrended, and thus zero mean, the AR model does not require an intercept. When the signal is purely random $e[k]$ is large, and a_1 is relatively small. As a system becomes progressively stressed, a_1 increases indicating increased recovery rates from stochastic disturbances. While higher order AR models can be used to gain additional information about the signal, we find that the first-order model provides good predictions of proximity to transition. The appendix includes some results for higher order models.

- 4) *Measure the variance (σ^2)* of the discrete detrended signal $d[k]$ using the same rolling window obtained in step 1. If there are n_k samples within the time window T , the variance is

$$\sigma^2 = \frac{1}{n_k} \sum_{k=1}^{n_k} d[k]^2. \quad (12)$$

As described in Section II-B, σ^2 tends to increase when systems approach critical transition. Thus, σ^2 is our second metric of proximity to critical transition.

- 5) *Test for statistical significance.* We test for statistically significant increases in a_1 and σ^2 using the nonparametric Kendall's τ coefficient [43]. Kendall's τ tests for serial dependence (i.e., a statistically significant increase) in a signal, against the null hypothesis that the signal is random. In our results we report τ_{a_1} and τ_{σ^2} for each one-minute interval before the transition.

In order to corroborate the findings from Kendall's τ , we also measure the power spectral density (PSD) of $d[k]$ using a Welch spectral estimator [44], which will show an increase in low-frequency components if the system is slowing down. The PSD of a signal can be found from the coefficients of higher order AR models and is thus related to the calculation of a_1 .

Based on prior research [25], [26], [45], we consider a system to be critically slowing if the variance and autocorrelation are significantly higher than "normal" values, and if Kendall's τ for each show a statistically significant upward trend. Practical implementation of this algorithm for power system operations would require that these two measures be observed under normal conditions for a period of time.

IV. RESULTS

This section discusses results from applying the method described in Section III to three test cases: a single-machine, stochastic infinite bus model (SMSIB), a three-machine nine-bus power system model (9 bus) [46] and data from the 10 August

1996 blackout in the Western North American Interconnection (WECC).

A. Single-Machine Stochastic-Infinite-Bus Model (SMSIB)

In our initial analysis, we modified the classic single machine infinite bus model ((3) and (4)) to determine the conditions under which critical slowing down appears in a power system model. In the stochastic version of the model, we gradually increase stress by linearly increasing the mechanical power of the generator P_m . To inject noise, we add noise to the infinite bus voltage (V_2 , with angle 0). We model the noise as a bandwidth-limited Gaussian white noise, where the voltage at Bus 2 is:

$$V_2(t_k) = 1.0 + \mathcal{N}(0, \sigma_V) \forall t_k \in \{0, 0.1, 0.2, \dots\} \quad (13)$$

and \mathcal{N} is a Gaussian random variable of zero mean and standard deviation σ_V . Between the discrete, 100 ms noise time steps, $V_2(t)$ is interpolated using a cubic spline. The noise magnitude σ_V is set to 0.01 p.u. The stochastic infinite bus simulates the effect of small, exogenous voltage flicker in the larger system to which the generator is connected [47]. A similar model, with noise in the generator power rather than the infinite bus voltage, is explored in [48].

The remaining set of parameters inherited from the classic SMIB model are set as follows: $E_a = 1.1$ p.u., $X_d = 0.1$, $D = 1.5$ p.u., $M = 3$ p.u. and $Z_{12} = j0.1$ p.u. The trajectories of δ and θ_1 are calculated using a variable step size, explicit trapezoidal differential-algebraic equation solver [49]. The output data from the DAE solver (most notably $|V(t)|$ and $\theta_1(t)$) are subsequently sampled at 30 Hz to obtain simulated synchrophasor data.

Critical slowing down becomes apparent in this model in several ways. As the dominant frequency of the system decreases, the relaxation time will increase, which is a symptom of CSD. Also, as the system approaches the point of transition, small changes in δ or in the noise (V_2) will substantially change the dominant frequencies in the system, resulting in a wider range of frequencies being present in the signal. This phenomena is sometimes apparent as flicker, which is another sign of CSD. Both of these phenomena can be observed in the power spectral density of the signal as an increase in the power of lower-frequency components, as well as an increase in the order 1 AR coefficient.

Fig. 3 shows the results that emerge from the two bus model as it is forced toward the maximum power transfer limit. Providing evidence in support of our conjecture that CSD is present before the critical transition, the order 1 AR coefficient (a_1) and variance (σ^2) in the phase angle data at Bus 1 increase notably minutes before the system hits the point of maximum power transfer. Kendall's τ (Table I) indicates that these increases are statistically significant. Furthermore the power spectral density of the signal (middle panel in Fig. 3) shows substantial increases in low-frequency signal power, relative to the power of the noise, as the system approaches the critical transition.

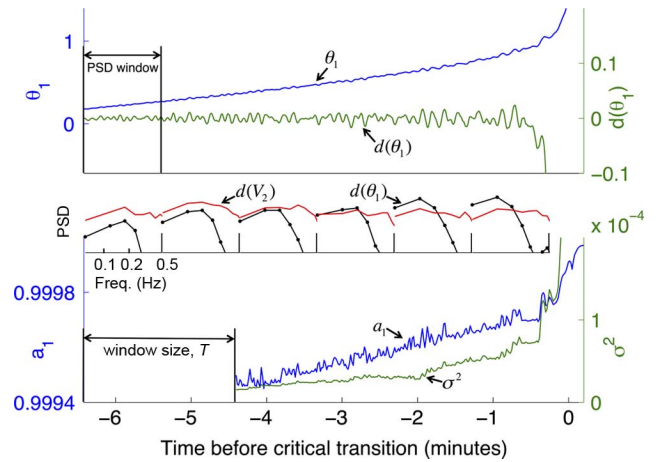


Fig. 3. Evidence of critical slowing down in a two-bus (SMSIB) power grid model being driven toward the point of maximum power transfer. The top panel shows the bus 1 voltage phase angle θ_1 before and after detrending. The middle panel shows the power spectral density of the detrended signal and the input noise for vertically projected time intervals. The lower panel shows the first order autoregression coefficient and the signal variance.

TABLE I
KENDALL'S τ , AND SIGNAL-TO-NOISE RATIOS FROM THE SMSIB MODEL

	Time range for τ calculation			
	$(-4, -3]$	$(-3, -2]$	$(-2, -1]$	$(-1, 0]$
τ_{a_1}	0.6294*	0.6000*	0.5344*	0.6384*
τ_{σ^2}	0.6814*	0.0525	0.8087*	0.8395*
SNR [0-0.15 Hz]	0.7747	1.7181	3.4764	7.2975

(* indicates that τ is statistically significant at the $P < 0.0001$ level.

B. Three-Machine, Nine-Bus Power System Model (9 Bus)

As a classic example multi-machine system, we utilize the Anderson and Fouad nine-bus test case [46] for the second set of experiments. The generators were modeled with order IV machines controlled by IEEE Type II exciters and turbine governors. As in Section IV-A, we injected bandwidth-limited Gaussian white noise into the system; in this case perturbing the loads. In order to stress the system and drive it toward a bifurcation, we steadily increase the baseline load and calculate the DAE trajectories with fixed a 1 ms time-step trapezoidal integration (using the PSAT simulator [50]). The output variables are subsequently sampled at 30 Hz. Fig. 4 illustrates the results of applying the CSD detection method to the nine-bus case. As with the single machine case, evidence of CSD is present minutes before the critical transition occurs.

These initial results indicate that when CSD is apparent, the stressed system processes noise differently than would a less-stressed one. In order to illustrate this, we represent the 9-bus system with the set of DAEs:

$$\begin{aligned} \frac{dx}{dt} &= \mathbf{f}(\mathbf{x}, \mathbf{y}) \\ \mathbf{0} &= \mathbf{g}(\mathbf{x}, \mathbf{y}) \end{aligned} \quad (14)$$

where \mathbf{x} are the state variables and \mathbf{y} are the algebraic variables (voltages). If we linearize the system we can obtain the following state-space matrix:

$$\mathbf{A} = \frac{d\mathbf{g}}{d\mathbf{y}} - \frac{d\mathbf{g}}{d\mathbf{x}} \left(\frac{d\mathbf{f}}{d\mathbf{x}} \right)^{-1} \frac{d\mathbf{f}}{d\mathbf{y}}$$

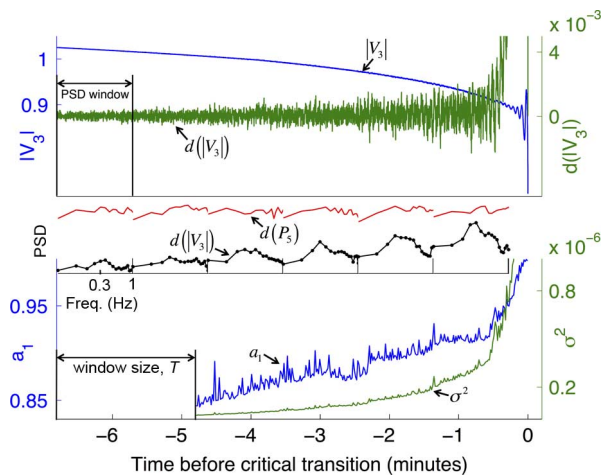


Fig. 4. Evidence of critical slowing down in a three-machine, nine-bus power grid model being driven toward a bifurcation. The top panel shows the bus 3 voltage magnitude $|V_3|$ before and after detrending. The middle panel shows the power spectral density of the detrended signal and the input noise for vertically projected time intervals. The lower panel shows the first order AR coefficient and the signal variance.

TABLE II

KENDALL'S τ , AND SIGNAL-TO-NOISE RATIOS FOR THE 9-BUS CASE

	Time range for τ calculation			
	$(-4, -3]$	$(-3, -2]$	$(-2, -1]$	$(-1, 0]$
τ_{a_1}	0.5277*	0.4055*	0.6240*	0.7853*
τ_{σ^2}	0.8407*	0.8251*	0.8514*	0.9356*
SNR [0-0.3Hz]	0.0011	0.0013	0.0058	2.0293

which can be interpreted as the dynamic power flow sensitivity matrix [50]. The frequency response of the 9 bus network can be observed by selecting the combination of input and output channels. Fig. 5 shows the magnitude response of $|V_3|$ to a noisy load connected at Bus 5 (P_5), for a high load and a low load case. At high load, the network is less able to damp out noise over a broad range of frequencies.

In order to illustrate how an aggregated measure derived from our four CSD indicators would be useful in assisting real time decisions, we performed the following experiment. First, we randomly generated 120 different load cases for 9 bus model. In each case the load at the three load buses increased at a different rate (between 21% and 27% per minute). The first 100 cases were used to calibrate a combined metric of proximity to transition, and the last 20 were used to test the metric. The data from the calibration cases were used to construct a multivariate regression model, as shown in (15). The output of the model (\hat{T}_i) is the estimated time to blackout in seconds. At a given time the predictors are $X_i = [a_{1,i}, \tau_{a_{1,i}}, \sigma_i^2, \tau_{\sigma^2,i}]$.

$$\ln(\hat{T}_i) = b_0 + b_1 \ln(a_{1,i}) + b_2 \ln(\tau_{a_{1,i}}) + b_3 \ln(\sigma_i^2) + b_4 \ln(\tau_{\sigma^2,i}). \quad (15)$$

The resulting regression coefficients from 100 training simulations were $b_0 = -7.601$, $b_1 = -5.305$, $b_2 = -0.084$, $b_3 = -0.732$, $b_4 = 0.396$.

Finally, in order to test the model in (15) we measured each of a_1 , τ_{a_1} , σ^2 , τ_{σ^2} for each second during the last 3 min before the transition for the 20 test cases, and used (15) to estimate the time until the critical transition. Fig. 6 shows the mean, 10th,

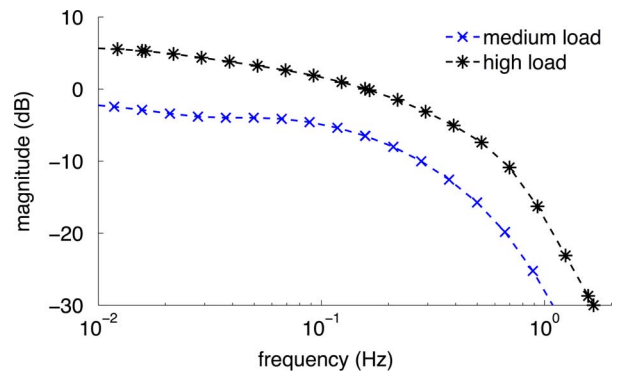


Fig. 5. Bode plot showing the magnitude response of the voltage magnitude at bus 3 to a load noise at bus five in the 9 bus power network for a high and a low load case. When the system is stressed, it is less able to damp out noise across a wide range of frequencies.

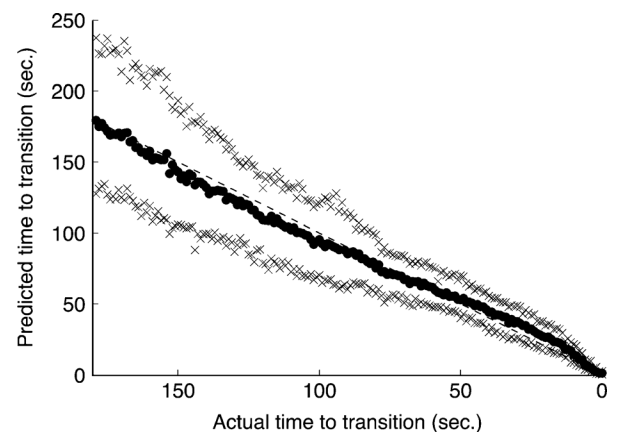


Fig. 6. Predicted distance to critical transition for 20 load stress scenarios of the three-machine, nine-bus (NB) model. Solid dots represent the mean output of the multivariate regression model for the set of test scenarios. The cross markers represent the percentile 10 (lower line) and 90 (upper line) outputs of the model for the set of test scenarios. The dashed line represents a perfect prediction.

and 90th percentiles for the 20 test runs. Samples with negative τ were not included in the figure. As the critical transition approaches, this simple regression model provides a good estimate of the distance between the current operating point and the critical transition. It is certainly possible that more sophisticated models would yield a better prediction. However, the fact that good predictions resulted from the simple model provides evidence that this approach is useful.

C. Western Interconnect Blackout of August 1996 (WECC)

On 10 August 1996 a long sequence of events resulted in the separation of the North America Western Interconnection into five sub-grids and the interruption of electric service to 7.5 million customers. [51] describes the sequence of events leading up to the blackout, and [52] provides a detailed analysis of the power system dynamics during the event. In [51], the WSCC (now WECC) disturbance study committee provided about 10 min of measured bus voltage frequency data from the Bonneville Power Administration territory, up until the point of separation. In order to test for CSD in these data, the printed frequency charts were scanned and translated into a numerical time series and the tests described above were repeated. As was found with the two and nine bus models, the order 1 autoregression

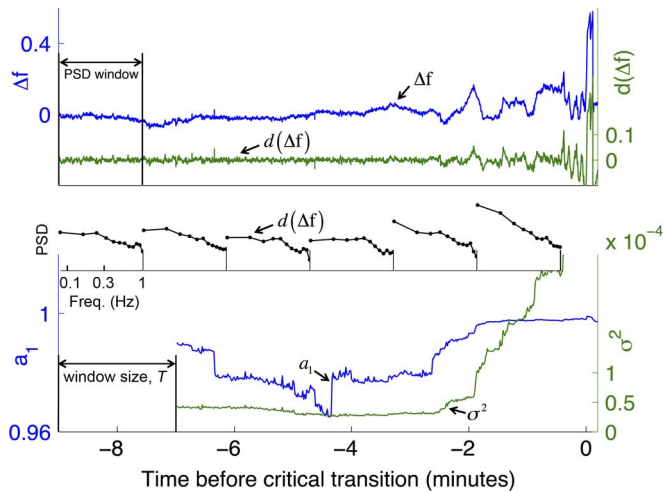


Fig. 7. Evidence of critical slowing down in the frequency as measured at the Bonneville Power Administration, immediately before the blackout of 10 August 1996. As in Figs. 3 and 4, the low-frequency components of the signal (middle panel) increase notably immediately before the transition occurs. In this case, our “distance to critical transition” model (see (15)) would predict the blackout 3 min before the major separation.

TABLE III
KENDALL’S τ FOR THE WECC CASE

	Time range for τ calculation			
	$(-4, -3]$	$(-3, -2]$	$(-2, -1]$	$(-1, 0]$
τ_{a_1}	0.5452*	0.8536*	0.7399*	0.4306*
τ_{σ^2}	0.5812*	0.7705*	0.9311*	0.8623*

coefficient and variance in the frequency signal increase significantly as the critical transition approaches, as does the density of low frequency changes (See Fig. 7). Kendall’s τ shows that the increases in autocorrelation are statistically significant.

V. CONCLUSIONS

This paper describes a method for estimating the proximity of a given power system operating point to a point of critical transition (which would typically lead to instability). The proposed predictor is unique in that it is based solely on the measured variance and autocorrelation in a single stream of high sample-rate voltage data, such as would proceed from a synchronized phasor measurement unit. Because of the minimal computational requirements and the increased availability of PMU technology, our method can be easily deployed as a component of real-time energy management systems.

Theoretical and empirical results from the study of critical slowing down and stochastic fast-slow systems show that increases in variance and autocorrelation signal proximity to critical transitions in many complex systems. We find these same indicators in a single machine, two bus model, a nine bus model, and in data from the large Western U.S. disturbance of August, 1996. In the 9-bus model, the indicator predicted the temporal distance to critical transition with substantial accuracy, particularly as the critical transition approached. We also found that, as the size and complexity of the benchmark system increased, the predictive ability of the indicators increased. Unlike traditional stability methods, the proposed statistical approach does not rely on network models and could therefore be useful even if state

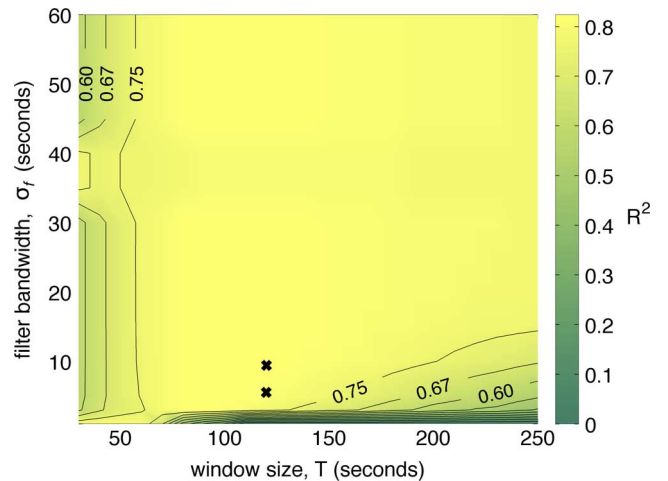


Fig. 8. The coefficient of determination, R^2 , for the predicted distance-to-transition values versus the empirical values given different ranges of parameters as inputs for the method described in Section III. The marked values at $T = 120$ s. and $\sigma_f = \{5, 10\}$ s. correspond to the experiments in Section IV.

estimators fail, so long as the operator has access to time-synchronized phasor data. Our method is also robust against faulty data from PMUs, assuming that latency and null samples from PMU data can be detected and filtered out of the noise streams. In the future, as more PMU data become available, this approach may be improved with the simultaneous use of multiple data streams. Additionally, an improvement of the detrending method to filter out discrete events could be used to remove discrete jumps in the data, such as those that would result from line tripping or islanding. The remaining signal could be tested for CSD without being biased by the spurious signals resulting from discrete changes.

It is important to note that the proposed proximity indicator, because it is statistical, does not indicate with certainty whether a given operating trajectory will result in instability. In order to transform the proposed analog indicator into a binary alarm, one would need to calibrate the alarm using historical PMU data to adjust for the local operators’ tolerance for false positive and false negative errors.

While the general approach described here is simple, the results suggest that it is feasible to obtain useful real-time information about distance to instability from a small quantity of time-series synchrophasor data.

APPENDIX

The CSD identification method that this paper proposes requires the selection of a few parameters that depend on the specific nature of the dynamical system in question. Steps 1 and 2 of the algorithm (Section III) make use of two of these parameters: the window size (T) and the GKS filter width (σ_f). This appendix describes results from sensitivity analysis on the 120 transition test runs shown in Fig. 6. For each of the 120 cases we computed the coefficient of determination R^2 for a range of values for T and σ_f (see Fig. 8).

Lastly, we studied the impact of using the first order autoregression models instead of higher order models. Fig. 9 illustrates that the first order autoregression coefficient shows similar trends relative to the higher order coefficients. Both the first

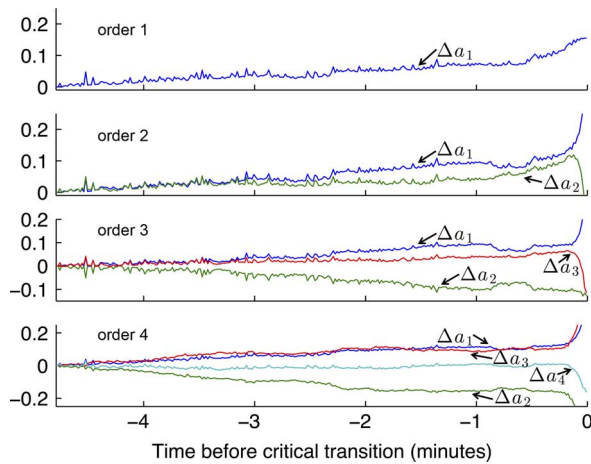


Fig. 9. Higher order autoregression coefficients corresponding to the nine-bus, three machine scenario experiment in Section IV-B (see also Fig. 4).

and higher order coefficients identify a shift in signal power from higher frequencies toward lower frequencies.

ACKNOWLEDGMENT

The authors gratefully acknowledge three anonymous reviewers for numerous helpful suggestions, Ian Dobson for comments on our method, and colleagues in the Vermont Complex Systems Center, who have encouraged development of these ideas.

REFERENCES

- [1] S. Abraham and J. Eford, "Final report on the August 14, 2003 blackout in the United States and Canada," US-Canada Power System Outage Task Force, 2004.
- [2] J. Medina, "Human error investigated in California blackout's spread to six million," *NY Times*, p. A15, Sep. 10, 2011.
- [3] G. A. Maas, M. Bial, and J. Fijalkowski, "Final report—System disturbance on 4 November 2006," Union for the Coordination of Transmission of Electricity in Europe, 2007.
- [4] A. Barrionuevo, "Officials search for answers in extensive Brazil blackout," *NY Times*, p. A6, Nov. 12, 2009.
- [5] I. Dobson, "Observations on the geometry of saddle node bifurcation and voltage collapse in electrical power systems," *IEEE Trans. Circuits Syst. I, Fundam. Theory Appl.*, vol. 39, no. 3, pp. 240–243, Mar. 1992.
- [6] V. Ajjarapu and B. Lee, "Bifurcation theory and its application to nonlinear dynamical phenomena in an electrical power system," *IEEE Trans. Power Syst.*, vol. 7, no. 1, pp. 424–431, 1992.
- [7] H. Chiang, I. Dobson, R. Thomas, J. Thorp, and L. Fekih-Ahmed, "On voltage collapse in electric power systems," *IEEE Trans. Power Syst.*, vol. 5, no. 2, pp. 601–611, 1990.
- [8] V. Venkatasubramanian, H. Schattler, and J. Zaborsky, "Dynamics of large constrained nonlinear systems—a taxonomy theory," *Proc. IEEE*, vol. 83, no. 11, pp. 1530–1561, 1995.
- [9] I. Dobson, J. Zhang, S. Greene, H. Engdahl, and P. Sauer, "Is strong modal resonance a precursor to power system oscillations?," *IEEE Trans. Circuits Syst. I, Fundam. Theory Appl.*, vol. 48, no. 3, pp. 340–349, 2002.
- [10] X. Wen and V. Ajjarapu, "Application of a novel eigenvalue trajectory tracing method to identify both oscillatory stability margin and damping margin," *IEEE Trans. Power Syst.*, vol. 21, no. 2, pp. 817–824, 2006.
- [11] H. Ghasemi, C. Canizares, and A. Moshref, "Oscillatory stability limit prediction using stochastic subspace identification," *IEEE Trans. Power Syst.*, vol. 21, no. 2, pp. 736–745, 2006.
- [12] D. Yang and V. Ajjarapu, "Critical eigenvalues tracing for power system analysis via continuation of invariant subspaces and projected arnoldi method," *IEEE Trans. Power Syst.*, vol. 22, no. 1, pp. 324–332, 2007.
- [13] Y. Susuki and I. Mezic, "Nonlinear Koopman modes and coherency identification of coupled swing dynamics," *IEEE Trans. Power Syst.*, no. 99, p. 1, 2011.
- [14] C. Taylor, D. Erickson, K. Martin, R. Wilson, and V. Venkatasubramanian, "WACS-wide-area stability and voltage control system: R&D and online demonstration," *Proc. IEEE*, vol. 93, no. 5, pp. 892–906, 2005.
- [15] J. De La Ree, V. Centeno, J. Thorp, and A. Phadke, "Synchronized phasor measurement applications in power systems," *IEEE Trans. Smart Grid*, vol. 1, no. 1, pp. 20–27, 2010.
- [16] T. Overbye, P. Sauer, C. DeMarco, B. Lesieutre, and M. Venkatasubramanian, "Using PMU data to increase situational awareness," PSERC, Tech. Rep. 10–16, 2010.
- [17] N. Senroy, "Generator coherency using the Hilbert-Huang transform," *IEEE Trans. Power Syst.*, vol. 23, no. 4, pp. 1701–1708, 2008.
- [18] I. Dobson, "Voltages across an area of a network," *IEEE Trans. Power Syst.*, 2012.
- [19] K. Sun, S. Lee, and P. Zhang, "An adaptive power system equivalent for real-time estimation of stability margin using phase-plane trajectories," *IEEE Trans. Power Syst.*, vol. 26, pp. 915–923, 2011.
- [20] Z. Zhong, C. Xu, B. Billian, L. Zhang, S.-J. Tsai, R. Conners, V. Centeno, A. Phadke, and Y. Liu, "Power system frequency monitoring network (FNET) implementation," *IEEE Trans. Power Syst.*, vol. 20, no. 4, pp. 1914–1921, Nov. 2005.
- [21] J. Ma, P. Zhang, H. Jun Fu, B. Bo, and Z. Yang Dong, "Application of phasor measurement unit on locating disturbance source for low-frequency oscillation," *IEEE Trans. Smart Grid*, vol. 1, no. 3, pp. 340–346, Dec. 2010.
- [22] B. Zeng, Z. Teng, Y. Cai, S. Guo, and B. Qing, "Harmonic phasor analysis based on improved FFT algorithm," *IEEE Trans. Smart Grid*, vol. 2, no. 1, pp. 51–59, Mar. 2011.
- [23] W. Gao and J. Ning, "Wavelet-based disturbance analysis for power system wide-area monitoring," *IEEE Trans. Smart Grid*, vol. 2, no. 1, pp. 121–130, Mar. 2011.
- [24] I. Sadinezhad and V. Agelidis, "Slow sampling online optimization approach to estimate power system frequency," *IEEE Trans. Smart Grid*, vol. 2, no. 2, pp. 265–277, Jun. 2011.
- [25] M. Scheffer, J. Bascompte, W. A. Brock, V. Brovkin, S. R. Carpenter, V. Dakos, H. Held, E. H. v. Nes, M. Rietkerk, and G. Sugihara, "Early-warning signals for critical transitions," *Nature*, vol. 461, pp. 53–59, 2009.
- [26] V. Dakos, M. Scheffer, E. H. v. Nes, V. Brovkin, V. Petoukhov, and H. Held, "Slowing down as an early warning signal for abrupt climate change," *Proc. Natl. Acad. Sci.*, vol. 105, no. 38, pp. 14 308–14 312, 2008.
- [27] J. Drake and B. Griffen, "Early warning signals of extinction in deteriorating environments," *Nature*, vol. 467, no. 7314, pp. 456–459, 2010.
- [28] P. McSharry, L. Smith, and L. Tarassenko, "Prediction of epileptic seizures: Are nonlinear methods relevant?," *Nat. Med.*, vol. 9, no. 3, pp. 241–242, 2003.
- [29] R. May, S. Levin, and G. Sugihara, "Ecology for bankers," *Nature*, vol. 451, no. 21, pp. 893–895, 2008.
- [30] D. Fisher, "Scaling and critical slowing down in random-field ising systems," *Phys. Rev. Lett.*, vol. 56, no. 5, pp. 416–419, 1986.
- [31] C. Kuehn, "A mathematical framework for critical transitions: bifurcations, fast-slow systems and stochastic dynamics," *Physica D: Non-linear Phenomena*, 2011.
- [32] C. Kuehn, "A mathematical framework for critical transitions: normal forms, variance and applications," *Arxiv Preprint*, 2011, ArXiv:1101.2908.
- [33] C. Canizares, "On bifurcations, voltage collapse and load modeling," *IEEE Trans. Power Syst.*, vol. 10, no. 1, pp. 512–522, 1995.
- [34] P. Kundur, *Power System Stability and Control*. New York: Electric Power Research Institute/McGraw-Hill, 1993.
- [35] C. Kuehn, "From first Lyapunov coefficients to maximal canards," *Int. J. Bifurcation Chaos*, vol. 20, no. 5, pp. 1467–1475, 2010.
- [36] V. Venkatasubramanian, H. Schattler, and J. Zaborsky, "Voltage dynamics: Study of a generator with voltage control, transmission, and matched mw load," *IEEE Trans. Autom. Control*, vol. 37, no. 11, pp. 1717–1733, 1992.
- [37] W. Ji and V. Venkatasubramanian, "Dynamics of a minimal power system: Invariant tori and quasi-periodic motions," *IEEE Trans. Circuits Syst. I, Fundam. Theory Appl.*, vol. 42, no. 12, pp. 981–1000, 1995.

- [38] C. Canizares, N. Mithulananthan, A. Berizzi, and J. Reeve, "On the linear profile of indices for the prediction of saddle-node and limit-induced bifurcation points in power systems," *IEEE Trans. Circuits Syst. I, Fundam. Theory Appl.*, vol. 50, no. 12, pp. 1588–1595, 2003.
- [39] C. Canizares, "Voltage stability assessment: Concepts, practices and tools," IEEE-PES Power System Stability Subcommittee, Special Publ. SP101PSS, 2002.
- [40] J. Guckenheimer and P. Holmes, *Nonlinear Oscillations, Dynamical Systems, and Bifurcations of Vector Fields*. New York: Springer-Verlag, 1990, vol. 42.
- [41] C. De Marco and A. Bergen, "A security measure for random load disturbances in nonlinear power system models," *IEEE Trans. Circuits Syst.*, vol. CAS-34, no. 12, pp. 1546–1557, 1987.
- [42] N. Zhou, D. Trudnowski, J. Pierre, S. Sarawgi, and N. Bhatt, "An algorithm for removing trends from power-system oscillation data," in *Proc. 2008 IEEE Power Energy Soc. Gen. Meet.—Convers. Del. Electr. Energy 21st Century.*, 2008, pp. 1–7.
- [43] T. Ferguson, C. Genest, and M. Hallin, "Kendall's tau for serial dependence," *Can. J. Stat.*, vol. 28, no. 3, pp. 587–604, 2000.
- [44] P. Welch, "The use of fast Fourier transform for the estimation of power spectra: A method based on time averaging over short, modified periodograms," *IEEE Trans. Audio Electroacoust.*, vol. AU-15, no. 2, pp. 70–73, 1967.
- [45] C. Meisel and C. Kuehn, "Scaling effects and spatio-temporal multilevel dynamics in epileptic seizures," *PLoS ONE*, vol. 7, no. 2, p. E30371, 2000.
- [46] P. Anderson and A. Fouad, *Power System Control and Stability*. Ames, IA: Iowa State Univ. Press, 1977.
- [47] R. Wiltshire, G. Ledwich, and P. O'Shea, "A Kalman filtering approach to rapidly detecting modal changes in power systems," *IEEE Trans. Power Syst.*, vol. 22, no. 4, pp. 1698–1706, 2007.
- [48] D. Wei and X. Luo, "Noise-induced chaos in single-machine infinite-bus power systems," *Europhys. Lett.*, vol. 86, p. 50008, 2009.
- [49] L. Shampine, M. Reichelt, and J. Kierzenka, "Solving index-i DAEs in MATLAB and simulink," *SIAM Rev.*, vol. 41, no. 3, pp. 538–552, 1999.
- [50] F. Milano, "An open source power system analysis toolbox," *IEEE Trans. Power Syst.*, vol. 20, no. 3, pp. 1199–1206, 2005.
- [51] "Western Systems Coordinating Council disturbance report for the power system outages that occurred on the Western Interconnection on July 2, 1996 and July 3, 1996," WSCC Operations Committee, Western Systems Coordinating Council, 1996.
- [52] V. Venkatasubramanian and Y. Li, "Analysis of 1996 Western American electric blackouts," *Proc. Bulk Power Syst. Dyn. Control—VI*, Aug. 2004.



Eduardo Cotilla-Sanchez (S'08–M'12) received the M.S. and Ph.D. degrees in electrical engineering from the University of Vermont, Burlington, in 2009 and 2012, respectively.

He is currently an Assistant Professor in the School of Electrical Engineering and Computer Science at Oregon State University, Corvallis. His primary field of research is the vulnerability of electrical infrastructure, in particular, the study of cascading outages.



Paul D. Hines (S'96–M'07) received the B.S. degree in electrical engineering from the University of Washington, Seattle, in 1997, the M.S. degree in electrical engineering from Seattle Pacific University, Seattle, WA, in 2001, and the Ph.D. degree in engineering and public policy from Carnegie Mellon University, Pittsburgh, PA, in 2007.

He is currently an Assistant Professor in the School of Engineering at the University of Vermont, Burlington, and a Member of the Adjunct Research Faculty at the Carnegie Mellon Electricity Industry center.

Formerly he worked at the U.S. National Energy Technology Laboratory, where he participated in smart grid research, the U.S. Federal Energy Regulatory Commission, where he studied interactions between nuclear plants and grid reliability, Alstom ESCA, where he worked on short-term load forecasting, and Black and Veatch, where he was involved with substation design projects.

Dr. Hines currently serves as the Vice-Chair of the IEEE Task Force on Understanding, Prediction, Mitigation and Restoration of Cascading Failures.



Christopher M. Danforth received the B.S. degree in math and physics from Bates College, Lewiston, ME, in 2001, and the Ph.D. degree in applied mathematics and scientific computation from the University of Maryland, College Park, in 2006.

He is currently on the faculty of the University of Vermont, Burlington, where he combines mathematical modeling and big data to study a variety of complex biological, natural, and physical systems. Among other projects, he has applied principles of chaos theory to improve weather forecasts, and

developed a real-time remote sensor of global happiness using Twitter. His research has been covered by the *New York Times*, *Science*, and the BBC among others. Descriptions of his projects are available at his website: <http://uvm.edu/cdanfort>